International Journal of Nanomedicine

Dovepress
open access to scientific and medical research

Open Access Full Text Article

ORIGINAL RESEARCH

Rhynchophylline Loaded-mPEG-PLGA Nanoparticles Coated with Tween-80 for Preliminary Study in Alzheimer's Disease

This article was published in the following Dove Press journal:
International Journal of Nanomedicine

Ruiling Xu[1]
Junying Wang[1]
Juanjuan Xu[1]
Xiangrong Song[2]
Hai Huang[2]
Yue Feng[3]
Chunmei Fu[1]

[1]Key Laboratory of Drug-Targeting and Drug Delivery System of the Education Ministry and Sichuan Province, Sichuan Engineering Laboratory for Plant-Sourced Drug and Sichuan Research Center for Drug Precision Industrial Technology, West China School of Pharmacy, Sichuan University, Chengdu 610041, People's Republic of China; [2]State Key Laboratory of Biotherapy/Geriatrics and Cancer Center, West China Hospital, Sichuan University, and Collaborative Innovation Center for Biotherapy, Sichuan University, Chengdu, People's Republic of China; [3]College of Pharmacy, Southwest University for Nationalities, Chengdu 610041, People's Republic of China

Purpose: Alzheimer's disease (AD) is a growing concern in the modern society. The current drugs approved by FDA are not very promising. Rhynchophylline (RIN) is a major active tetracyclic oxindole alkaloid stem from traditional Chinese medicine uncaria species, which has potential activities beneficial for the treatment of AD. However, the application of rhynchophylline for AD treatment is restricted by the low water solubility, low concentration in brain tissue and low bioavailability. And there is no study of brain-targeting therapy with RIN. In this work, we prepared rhynchophylline loaded methoxy poly (ethylene glycol)–poly (dl-lactide-co-glycolic acid) (mPEG-PLGA) nanoparticles (NPS-RIN), which coupled with Tween 80 (T80) further for brain targeting delivery (T80-NPS-RIN).

Methods: Preparation and characterization of T80-NPS-RIN were followed by the detection of transportation across the blood–brain barrier (BBB) model in vitro, biodistribution and neuroprotective effects of nanoparticles.

Results: The results indicated T80-NPS-RIN could usefully assist RIN to pass through the BBB to the brain. T80-NPS-RIN treatment regulated the activity of neurons in vitro.

Conclusion: The presented data confirmed that rhynchophylline encapsulated mPEG-PLGA nanoparticles coated with Tween 80 could across through the BBB and exhibited efficient neuroprotective effects. The T80-NPS-RIN nanoparticles have a chance to be an alternative drug to the therapy of AD.

Keywords: Alzheimer's disease, rhynchophylline, nanoparticles, blood–brain barrier, neuroprotective effect

Introduction

Nowadays, Alzheimer's disease (AD) is a serious social problem among the neurodegenerative diseases.[1] With the increasing incidence of AD, the prevention and treatment of AD has become a global focus. The neuropathological characteristics of AD mainly include age-related Aβ deposition, synapses and neuronal loss and neurofibrillary tangles.[2–4] Accumulated soluble Aβ-induced abnormal neuronal network activity has been considered to play a significant role in the development of AD.[5,6] At present, only five FDA-approved medicines are able to temporarily reduce AD symptoms.[7] Furthermore, it should be noticed that these approved drugs cannot cure or delay the progression of AD, but only improve some symptoms for a limited time.[8] Therefore, the development of new AD therapeutics agents is urgently needed.

Traditional Chinese medicine (TCM) has been used to prevent and treat cognitive decline.[9–11] The anti-AD agents from TCM have been developed for a long time.[12,13]

Correspondence: Chunmei Fu
Key Laboratory of Drug-Targeting and Drug Delivery System of the Education Ministry and Sichuan Province, Sichuan Engineering Laboratory for Plant-Sourced Drug and Sichuan Research Center for Drug Precision Industrial Technology, West China School of Pharmacy, Sichuan University, Chengdu 610041, People's Republic of China
Email fuchunmei@scu.edu.cn

submit your manuscript | www.dovepress.com
DovePress
http://doi.org/10.2147/IJN.S236922

Rhynchophylline (RIN) is a major active tetracyclic oxindole alkaloid stem from traditional Chinese medicine uncaria species.[14] RIN has been used commonly in the treatment of central nervous system diseases including hypertension, convulsions, stroke, as well as AD.[15] RIN has great potential in the treatment of AD because it could inhibit soluble Aβ-induced hyperexcitability of hippocampal neurons.[16,17]

Although RIN shows some good therapeutic effects in AD, its application is limited by its low solubility, low concentration in brain tissue and low bioavailability with low permeability through blood–brain barrier (BBB).[18,19] Nanotechnology-based drug delivery systems with good solubility, high bioavailability, less patient variability and prolonged circulation time provide new therapeutic strategy for AD with brain targeting TCM delivery across through the BBB.[20–22]

A substance assisting in targeting drug delivery into the brain is Tween 80 (polysorbate 80), which is commonly coating the surfaces of nanoparticles for drug load and delivery.[23] Tween 80 can adsorb apolipoprotein E and enable the binding to the lipoprotein receptor-related proteins (LRPs).[24] The nanoparticles coated Tween 80 can across through the BBB via LRPs mediated transcytosis.[25] The schematic diagram of T80-NPS-RIN crossing BBB is shown in Figure 1. In this work, we utilized methoxy poly (ethylene glycol)–poly (dl-lactide-co-glycolic acid) (mPEG-PLGA) nanoparticles for the load of RIN with prolonged blood residence. Rhynchophylline loaded in mPEG-PLGA nanoparticles coated with Tween 80 was investigated and preliminarily evaluated for treatment of AD in cell model in vitro. T80-NPS-RIN exhibited increased therapeutic efficacy against nerve injury with high concentration of rhynchophylline accumulation in brain and higher bioavailability.

Materials and Methods

Materials

Rhynchophylline (purity>98%) was purchased from Beisite Biotechnology Co., Ltd. (Chengdu, China). For in vitro cell studies, rhynchophylline was dissolved in dimethyl sulfoxide (DMSO) and further diluted in culture medium (DMEM with 10% fetal bovine serum) to the required concentration with the final concentration of

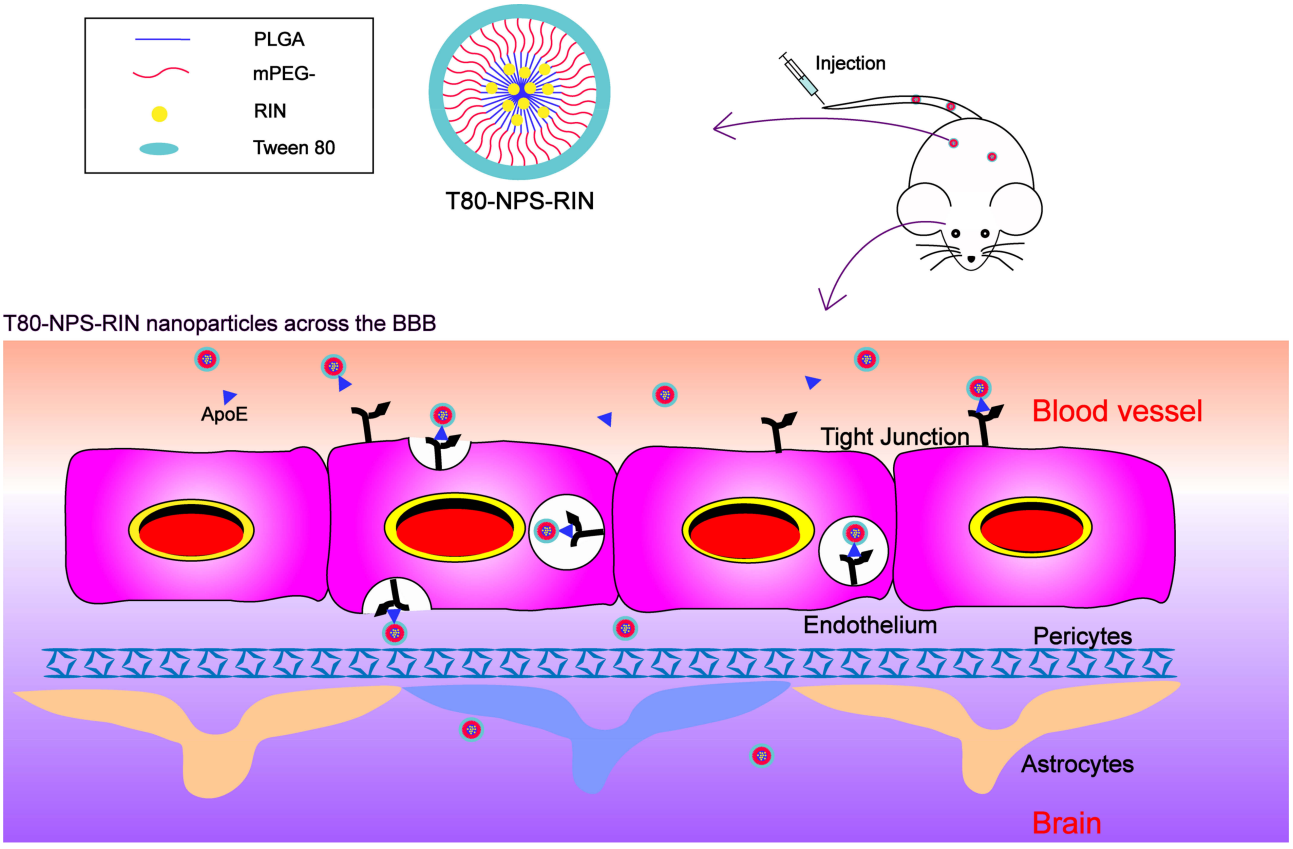

Figure 1 Diagrammatical representation of T80-NPS-RIN cross BBB. Intravenously administered nanoparticles went to the brain and cross the BBB due to apolipoprotein E (ApoE) receptor-mediated transendocytosis.

DMSO concentration <0.1% (v/v). Cell culture plates and transwell plates were obtained from Corning INC. (Corning, NY, USA). Hoechst 33258 staining kit was purchased from Beyotime Biotechnology Co., Ltd. (Shanghai, China). mPEG-PLGA (MW = 15 kDa; LA/GA = 75:25; PEG MW = 2 kDa) was purchased from Jinan Daigang Biomaterial Co., Ltd. (Jinan, China). Poly (vinyl alcohol) (PVA, MW=30–70 kDa, HD, 80%), 3-[4,5-dimethylthiazole-2-yl]-2,5-diphenyltetrazolium bromide (MTT) and Tween 80 were purchased from Chengdu Real Biotechnology Co., Ltd. All other reagents were of analytical grade and were used as supplied.

Animals

C57BL/6 mice (aged 6–8 weeks, male and weighed 22–25 g, SPF grade) and adult healthy male Sprague-Dawley rats (body weight range 200–250 g, SPF grade) were purchased from Dashuo Biotechnology Company, Ltd. (Chengdu, Sichuan, China). All the experiments on animals were approved and supervised by the West China School of Pharmacy Animal Care and Use Committee (Sichuan University). All animals were kept in the environment of 12:12 hrs light–dark cycle at the temperature 22 ± 1°C and the relative humidity remained at 55 ± 10%.

Preparation of T80-NPS-RIN

RIN loaded mPEG-PLGA nanoparticles (NPS) were prepared by nanoprecipitation method using PVA as an aqueous phase. RIN (60 mg/mL) and mPEG-PLGA (120 mg/mL) in the ratio of 1:2 were dissolved in N,N-Dimethylformamide (DMF). The organic phase containing RIN (100 μL) and mPEG-PLGA (100 μL) mixture was added drop by drop to 2.5 mL of 1% PVA solution with continuous stirring (1200 rpm) on magnetic stirrer. Then, the NPS suspension was centrifuged at 2800 rpm for 15 mins at 4°C. Next, the suspension was washed with phosphate buffer saline (PBS) twice using high-speed centrifuge at 2800 rpm for 15 mins. Finally, 1% (w/v) of Tween 80 was added to the NPS solution at low-speed (400 rpm). And the mixture was stirred slowly at 400 rpm for 30 mins to facilitate T80-NPS-RIN formation. In the end, T80-NPS-RIN was acquired after the above process was filtered through hydrophilic filter membranes (pore size, 0.22 μm). Furthermore, the drug loading and encapsulation efficiency were measured by LC/MS analysis.

The drug loading and encapsulation efficiency (%) of nanoparticles were calculated according to the following equation:

$$\text{Drug load} = \frac{W_1}{W_2} \times 100\%$$

$$\text{Encapsulation efficiency} = \frac{W_3 - W_4}{W_3} \times 100\%$$

where W_1 is the weight of drug (RIN) in the nanoparticles, W_2 is the gross weight of nanoparticles, W_3 is the total weight of drug, and W_4 is the weight of drug (RIN) that remained in the liquid medium after encapsulation.

Particle Size and TEM Analysis

The particle size and polydispersity index (PDI) were analyzed using a Mastersizer (Zetasizer NanoZS 90). The tested samples were diluted 10 times for measurements. Each sample was measured three times in parallel. The morphology of the nanoparticles was observed using transmission electron microscopy (TEM) at 200 kV. For TEM analysis, 10 μL of the nanoparticle solution was spotted on the copper microgrid and waited for the solution to dry. After that, the data were obtained at an accelerating voltage.

In vitro Hemolysis Assay

Red blood cells (RBCs) of healthy rabbit were used for evaluating the hemolytic potential of T80-NPS-RIN. 2% of erythrocyte suspension was obtained by centrifuging the blood samples and re-dissolving in normal saline. Next, 2.5 mL of the erythrocyte dispersion solution was mixed with free RIN solution and nanoparticles with a total volume of 5 mL. Distilled water was employed as a positive control, and saline solution was employed for the negative control group. All tubes were incubated at 37°C for 3 hrs. Then, all the samples were centrifuged. The absorbance (A) of supernatant was examined at 570 nm by UV spectrophotometer. The hemolysis (%) of RBSs was calculated according to the following equation:

$$\text{Hemolysis}(\%) = \frac{\text{A}_{\text{sample}} - \text{A}_{\text{negative control}}}{\text{A}_{\text{positive control}} - \text{A}_{\text{negative control}}} \times 100\%$$

Cell Culture

Mouse brain endothelial cells bEnd.3 and highly differentiated mouse pheochromocytoma cells PC12 were obtained from American Type Culture Collection (ATCC). The cells were both cultured in the high-glucose DMEM medium containing 10% fetal bovine serum, 1% L-glutamine and 1% penicillin-streptomycin mixture. Cells were set in incubator at 37°C with humidified air involving 5% CO_2.

In vitro Uptake Study in bEnd.3 Cells

The internalization studies of NPS and T80-NPS-RIN in bEnd.3 cells were investigated using confocal laser-scanning microscopy (CLSM). As RIN is non-fluorescent, NPS-DiD and T80-NPS-DiD (the preparation method as before, DiD instead of RIN) were replaced for the assay. The bEnd.3 cells were grown on 15 mm glass base culture dishes at a concentration of 5×10^4 cells each plate for 24 hrs. After that, 500 μL of NPS-DiD and T80-NPS-DiD solution were added to the cultures and incubated for 3 hrs. After incubation, the bEnd.3 cells were rinsed with PBS buffer and re-suspended in 2 mL fresh medium. Finally, the cells were viewed using a high-speed confocal laser-scanning microscope (CLSM, Axio-Imager LSM-800) at excitation wavelengths of 345 nm (Hoechst) and 644 nm (DiD).

For flow cytometry studies, bEnd.3 cells were seeded into 24-well plates with a density of 6×10^3 cells per well. After adherence for 12 hrs, 25 μM of DiD, NPS-DiD and T80-NPS-DiD were added. After incubation for different times, bEnd.3 cells were trypsinized and washed twice with PBS buffer. Next, cells were resuspended in 300 μL PBS. The cellular uptake was assessed by flow cytometry (ACEA NovoCyte™) and the data were analyzed using Flowjo software.

Transportation Across the BBB Model in vitro

The BBB model in vitro was prepared using immortalized mouse brain endothelial cells (bEnd.3 cells). 7×10^3 bEnd.3 cells were cultured on the apical side of the insert to form the tight junction for 5–7 days. The medium of barrier was replaced with fresh medium every 2 days and cell growth was monitored every day. The integrity of the barrier was evaluated by testing the transendothelial electrical resistance (TEER) using cell resistance meter (Millicell-ERS EVOM2, USA). In order to ensure the accuracy of the values, the entire process was carried out at a constant temperature (25°C). Three points in different directions were taken for each cell insert and measured repeatedly for three times. Relative TEER = (sample reading of inoculated cells – blank control sample reading) × 0.33.

To evaluate the transportation of nanoparticles across the BBB model in vitro, the model was constructed by the culture of bEnd.3 cells for 7 days. Briefly, the cells were cultured on a pore size permeable polycarbonate filter insert with 12-mm-diameter transwell in fresh medium. The media was washed with sterile HBSS (Hank's balanced salt solution) before the addition of nanoparticles. Next, the cells preincubated in HBSS at 37°C for 20 mins in incubator. After that RIN, NPS-RIN and T80-NPS-RIN (25 μM) in 500 μL of fresh buffer containing serum were added to the apical side and 1500 μL HBSS was added to the basolateral side. Then, an aliquot of 100 μL was collected from the basolateral side and replace with fresh HBSS at different time intervals (0.5, 1, 2, 3 and 4.5 hrs). Finally, the aliquoted samples were used for LC/MS analysis.

Biodistribution Study

All of the C57BL/6 mice were fed a week to adapt the new environment, and they were investigated for organ biodistribution studies, which were randomly divided into three groups (n=5) and control groups (n=5). 200 μL of DiD, NPS-DiD and T80-NPS-DiD solution were injected into the healthy mice via the tail vein. As for the control group, same volume physiological saline was given to the mice. After 2 hrs, the mice were promptly killed and the organs (liver, heart, spleen, lung, kidney, and brain) were harvested and imaged via an FMT 4000 fluorescence tomography system in vivo imaging system to measure the fluorescence of the tested organs.

Pharmacokinetics of T80-NPS-RIN

In pharmacokinetic study, adult healthy male Sprague-Dawley rats (body weight range 200–250 g) were tested. Before the experiment, all animals were fasted overnight, but water was provided. Eighteen rats were randomly divided into three groups (n = 6 per group). Then, the NPS-RIN group, the T80-NPS-RIN group and the free RIN group (suspended in physiological saline) were administered at an equivalent dose of 1 mg/kg via the tail vein. According to the time points (5 mins, 15 mins, 30 mins, 1 hr, 2 hrs, 4 hrs and 8 hrs), blood samples (300 μL) were collected into 2 mL Eppendorf tube containing heparin sodium solution (20 mg/mL, 20 μL). Next, all blood samples were centrifuged at 3000 rpm for 10 mins followed by plasma separation. Some of the plasma sample (150 μL) was mixed with carbamazepine (internal standard, 10 μL) and vortexed for 30 s. Then, an aliquot of 300 μL acetonitrile was added and centrifugated at 12,000 rpm for 10 mins. Finally, the supernatant which was taken from treated samples was analyzed in LC/MS. Then, the pharmacokinetic parameters were estimated using statistical analytical tool Winnonlin.

Protection of T80-NPS-RIN on $A\beta_{25–35}$-Induced Cytotoxicity in PC12 Cells

$A\beta_{25–35}$ was dissolved in bacteria-free saline to the concentration of 1 mM and incubated at 37°C for 7 days to form fibril formation. After aggregation, the solution was conserved at −20°C until experiment.

PC12 cells were seeded at densities of 7×10^3 cells/well in 96-well plates. After culture for 24 hrs to make sure of adherence, $A\beta_{25–35}$ at several concentrations (0, 10, 20, 40 μM) dissolved in free-serum DMEM was added. After that, the cells continued to be cultured for 24 hrs. The MTT (5 mg/mL, dissolved in PBS) was added 20 μL to each well and incubated for 4 hrs at 37°C. Next, the supernatants were removed and purple crystal formazan were dissolved with 150 μL of DMSO. Then, the value of absorbance at 570 nm was measured using a microplate reader. In addition, the cells which were injured by $A\beta_{25–35}$ were analyzed by inverted microscope. The optimal concentration of $A\beta_{25–35}$ solution was 20 μM to use for the following experiment. PC12 cells were cultured for adherence as above, they were pretreated at different doses of RIN and T80-NPS-RIN (12.5 and 50 μM) for 4 h; then, the medium was discarded and 200 μL/well $A\beta_{25–35}$ was added. Cells were cultured for another 24 hrs in incubator at 37°C. Finally, the cells viability was tested by MTT assay as previously described.

Apoptosis Assay of T80-NPS-RIN Ability to Protect PC12 Cells Against $A\beta_{25–35}$ Injury

PC12 cells (6×10^3 per well) were seeded into a 24-well plates. Then, the cells were treated with RIN, NPS-RIN and T80-NPS-RIN (25 μM) for 24 hrs. Next, the medium was replaced by $A\beta_{25–35}$ solution (20 μM) for another 4 hrs. Subsequently, the PC12 cells were collected by trypsinization and washed twice with PBS and stained by Annexin V PE/7-AAD (BD Biosciences) for 15 mins at room temperature without light. The stained PC12 cells were analyzed using a flow cytometer. Experiments were performed in triplicates.

Results and Discussion

Characterization of T80-NPS-RIN

Particle Size and TEM Analysis

In order to enhance the pharmacological activity of RIN on Alzheimer's disease, RIN nanoparticles coated with Tween 80 was prepared. The drug loading and encapsulation efficiency of nanoparticles were 10.3% and 60%. The mean particle size of nanoparticles was 145.2 nm (Figure 2A) with PDI of 0.133. And the size and PDI both measured by Mastersizer. T80-NPS-RIN was observed with TEM and presented alike a sphere (Figure 2B), which is agreement to result measured by a Mastersizer.

Preliminary Evaluation of Safety

Tween 80 (polysorbate 80), is a kind of polyoxyethylene derivatives of nonionic surfactant. It is commonly used supplementary material in pharmaceutical preparations.[26] However, it has been reported that Tween 80 caused adverse reactions as a solution-enhancing medicinal excipient.[27] Thus, the safety of T80-NPS-RIN was preliminarily evaluated through the study of hemolysis assay in vitro. The results of the hemolysis assay are exhibited in Figure 2C. The results showed that hemolysis only occurred in the tube of distilled water. The hypotonic distilled water made erythrocytes rupture, resulting in hemolysis. Moreover, it was clear that no hemolysis occurred in the tubes which contained T80-NPS-RIN. And the hemolysis percentages in nanoparticle groups were all less than 5% (Figure 2D). These results indicated the preliminary safety of T80-NPS-RIN for intravenous injection administration.

Cellular Uptake Studies in bEnd.3 Cells

The cellular uptake image of NPS-DiD and T80-NPS-DiD in bEnd.3 cells at 3 hrs was investigated by CLSM (Figure 3A). Both NPS-DiD and T80-NPS-DiD showed a certain degree of cellular uptake. Additionally, compared with NPS-DiD, T80-NPS-DiD showed high cellular uptake in cells. It revealed that Tween 80 modified nanoparticles improved permeation. As for the results of flow cytometry, a time-dependent uptake was confirmed as Figure 3B displayed. The fluorescence intensity increased with incubation time, from 1.5 hrs to 7 hrs. T80-NPS-DiD was internalised in bEnd.3 cells with good uptake (Figure 3C). The mean fluorescence intensity (MFI) for bEnd.3 cells incubated with T80-NPS-DiD was significantly higher than NPS-DiD at 7 hrs (Figure 3B).

Permeability Studies

The integrity of blood–brain barrier was assessed by measuring TEER across the culture of bEnd.3 cells. The TEER values of the monolayer should be increasing along with the extension of the culture time. In this study, the TEER of the bEnd.3 cells was measured from the third day, and it was found that the TEER gradually increased as time went

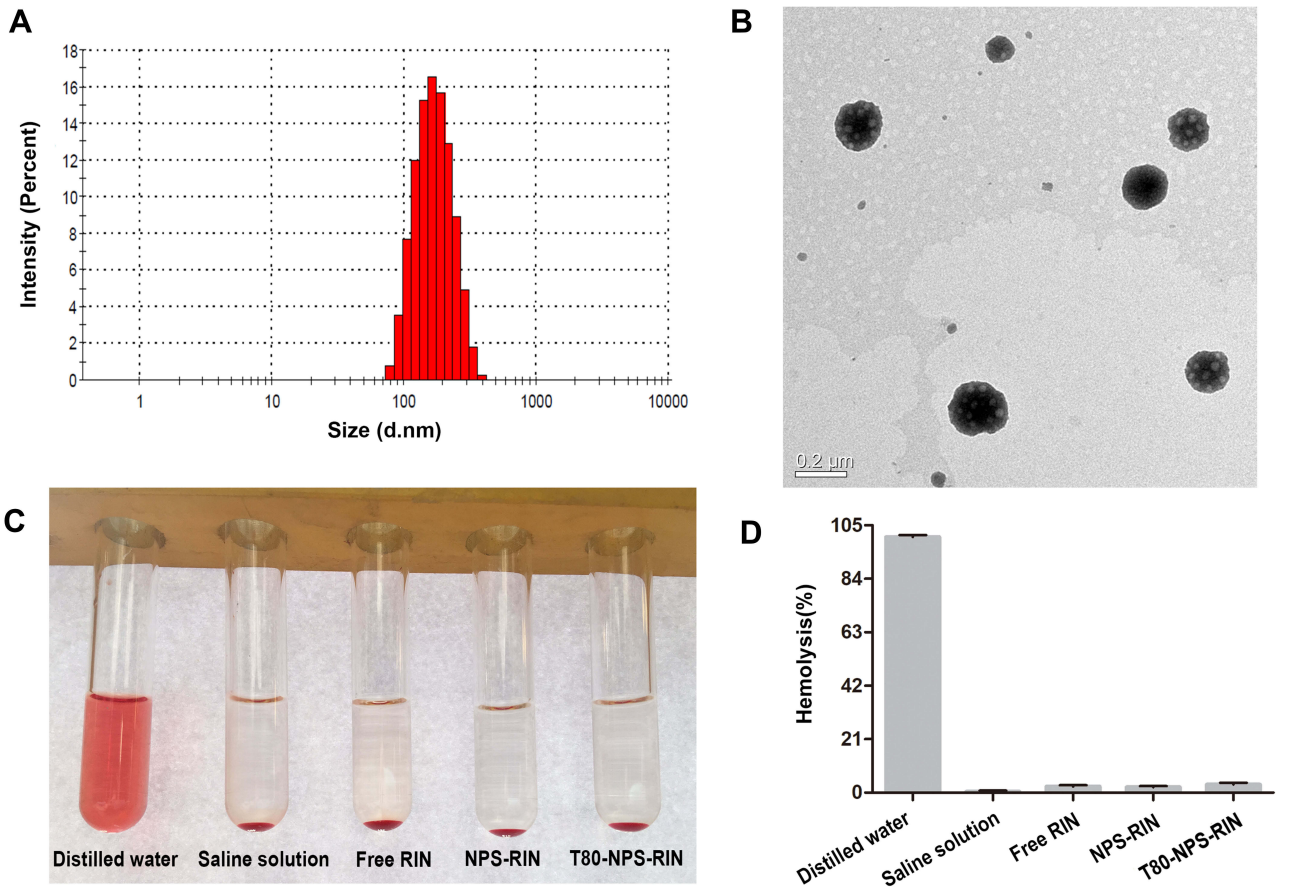

Figure 2 Characterization of T80-NPS-RIN. (**A**) The size distribution of T80-NPS-RIN obtained by Mastersizer. (**B**) The TEM image of T80-NPS-RIN. (**C**) Images of hemolysis on rabbit red blood cells of T80-NPS-RIN compared with free RIN solution, NPS-RIN. (**D**) The percentages of hemolysis (%) in each group.

on. What's more, the reading tended to stabilize at the fifth day. And the TEER value was around 100 $\Omega \cdot cm^2$ which was accorded with experimental results from Brown et al.[28] Furthermore, the TEER value was consistent with mostly the published TEER values of BMEC (brain microvascular endothelial cell) obtained from primary culture of each species.[29,30] This result showed that after 6 days of culture, bEnd.3 cells formed tight junction and had good limits on the permeability by exogenous molecules.

In this study, we build an in vitro BBB model (Figure 4A) to study the transport of T80-NPS-RIN across the endothelial barrier layer (bEnd.3 cells). As Figure 4B showed, T80-NPS-RIN demonstrated significantly higher transport across the in vitro BBB model as compared to RIN or NPS-RIN. With the increase of time, the drug accumulation increased, and reached permeability saturation after 3 hrs. Moreover, the TEER value fluctuated within the normal range (Figure 4C), indicating that the cell was always in a condition of tight connection.

Biodistribution Study

The brain-targeting capability of nanoparticles was studied in healthy C57BL/6 mice. As Figure 5A revealed, T80-NPS-DiD showed significant distribution in brain compared to free DiD and NPS-DiD. It denoted that T80-NPS was able to deliver the drug into the brain. Notably, the remarkable fluorescence sign (Figure 5B) in the brain suggested that the T80-NPS penetrated the BBB and presented in the mouse brain which tallied with the result of permeability studies in vitro. On the other hand, NPS coated without Tween 80 exhibited high aggregation in liver and spleen because of capturing by the reticuloendothelial system. In addition, NPS had no brain targeting effects indicating that the Tween 80 coating is important for the delivery of drugs into the brain. Meanwhile, many other studies were in favor of Tween 80′ s special status in the delivery of nanoparticles into the brain. They reported it was concerned that nanoparticles coated with tween 80 interacted with micro-vessel endothelial cells.[31] The present study showed the same

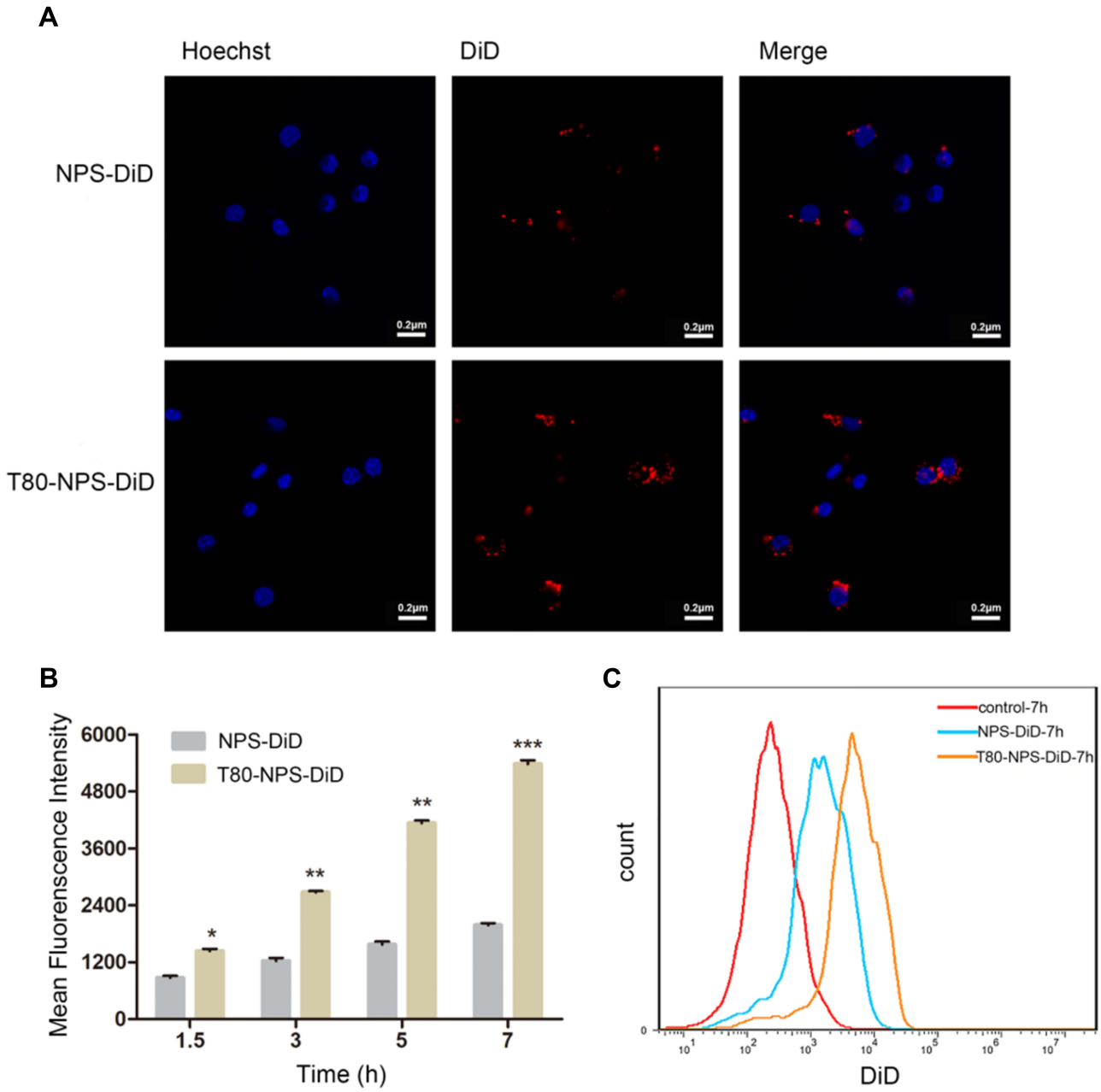

Figure 3 In vitro cellular uptake of T80-NPS-RIN. (**A**) CLSM images representing cellular uptake of NPS-DiD or T80-NPS-DiD at 3 hrs, red indicates NPS-DiD or T80-NPS-DiD while blue indicates the nucleus. (**B**) Mean DiD fluorescence intensity of bEnd.3 cells incubated with NPS-DiD or T80-NPS-DiD for 1.5, 3, 5, and 7 hrs. (**C**) Flow cytometry analysis of bEnd.3 cells treated with NPS-DiD or T80-NPS-DiD for 7 hrs. Data are shown as the mean ± SD; N = 3; *P < 0.05, **P < 0.01, and ***P <0.001 compared to the NPS-DiD groups.

result. In conclusion, the developed nanosystem (T80-NPS) was an applicable strategy for the delivery of RIN for AD therapy.

Pharmacokinetics

The correlative main pharmacokinetic parameters are displayed in Table 1. And the plasma concentration–time curve (Figure 6) of free RIN displayed a peak of 164.4 ng/mL after intravenous injection and then showed rapidly decrease. In contrast, the maximum plasma concentration (C_{max}) in NPS-RIN (536.3 ng/mL) and T80-NPS-RIN (673 ng/mL) group were remarkably higher in comparison with that of in RIN group. Furthermore, the area under the concentration–time curve (AUC) of T80-NPS-RIN was 412.63 ng/mL*h, which was approximately 3-fold higher than that of free RIN (136.06 ng/mL*h). Moreover, the

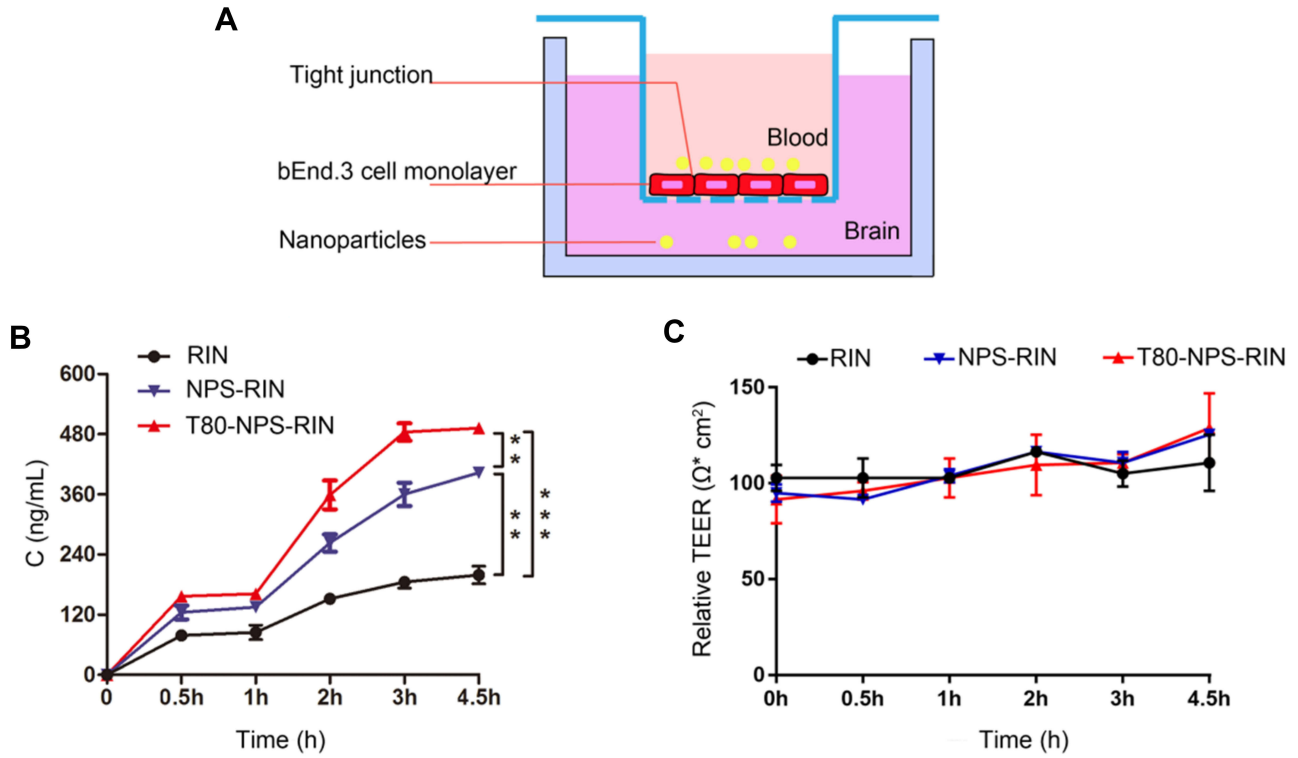

Figure 4 Transportation of RIN loaded nanoparticles across the BBB model in vitro. (**A**) The schematic diagram of BBB model in vitro. (**B**) Concentration cellular permeation of RIN when treated as a plain RIN solution, NPS-RIN, and T80-NPS-RIN on mouse brain endothelial (bEnd.3) cell monolayer. (**C**) The fluctuation of TEER value during the permeation experiment. Results are denoted as mean ± SD (n=3), **P < 0.01, and ***P <0.001.

clearance (Cl) of the T80-NPS-RIN (1938.76 mL/h/kg) was relatively slower than that of free RIN (5912.78 mL/h/kg), which showed relatively slow elimination from the blood circulation. The above pharmacokinetic results indicated that the metabolic processes of T80-NPS-RIN in vivo were different from free RIN.

Protection of PC12 Cells by T80-NPS-RIN from $A\beta_{25–35}$-Induced Cytotoxicity

To explore whether T80-NPS-RIN treatment could protect PC12 cells injured by $A\beta_{25–35}$, we used MTT and microscope assays to evaluate the cell viability. As Figure 7A showed, PC12 cells of the control group after 24 hrs of culture, exhibited complete cell morphology and obvious protrusions of different lengths. The picture showed the cells had no damage or fracture. As for the treatment group, $A\beta_{25–35}$ (Figure 7A) damaging cells became swollen, fractured, shortened, and globular. Apparently, the larger the concentration of $A\beta_{25–35}$, the greater the damage to the cells. According to MTT results (Figure 7B), the cell viability decreased with the concentration of $A\beta_{25–35}$ increased. 20 μM $A\beta_{25–35}$ which could lead to 50–60% cell death was selected to establish an AD model in vitro for the later experiments. As shown in Figure 7C, the T80-NPS-RIN group at different concentrations markedly reduced the cell death caused by $A\beta_{25–35}$ compared with the RIN group. It demonstrated T80-NPS-RIN could interfere with cell damage caused by $A\beta_{25–35}$ and improved cell survival rate. Besides that, as the concentration of T80-NPS-RIN increased, it had a strong protective effect on PC12 cells.

Effect of T80-NPS-RIN on $A\beta_{25–35}$-Induced Apoptosis in PC12 Cells

To investigate the effect of T80-NPS-RIN in $A\beta_{25–35}$-induced apoptosis, we utilized flow cytometer to measure the relative amounts of Annexin V PE/7-AAD stained cells. As the results showed in Figure 7D, with the treatment of Aβ solution, markedly increased apoptotic death in PC12 cells, with the total apoptotic effect reaching to 22.59%. Pre-treatment with RIN and NPS-RIN for 4 hrs prior to Aβ exposure decreased the apoptotic rate to 12.53% and 11.53%, respectively. Furthermore, pre-treatment with T80-NPS-RIN resulted in a dramatic reduction in the amount of cell apoptosis compared with the Aβ solution (Figure 7E), which decreased the apoptotic rate to 8.18%. Consistent with

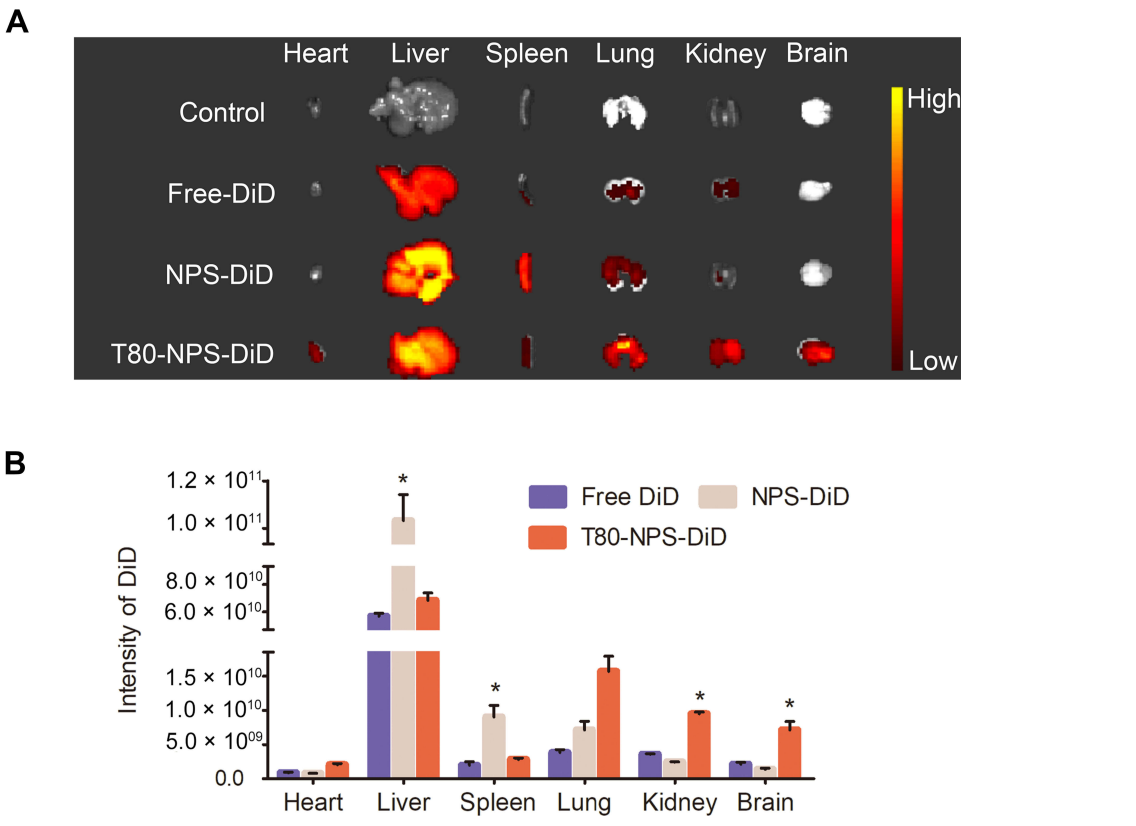

Figure 5 In vivo fluorescence images of free DiD, NPS-DiD or T80-NPS-DiD. (**A**) Representative fluorescent images of different vital organs and brains at 2 hrs after intravenous injection of the free DiD, NPS-DiD or T80-NPS-DiD. (**B**) Quantitative analysis of the intensity of fluorescence signal from free DiD, NPS-DiD or T80-NPS-DiD in each group of organs. *p < 0.05, compared to the free DiD groups.

the MTT results, these results suggested that T80-NPS-RIN could protect the injury by $A\beta_{25-35}$ solution in PC12 Cells.

Conclusions

A nanoparticle delivery system loading Rhynchophylline (RIN) was first developed to treat AD, which solved the problem of RIN's low solubility, low bioavailability and especially low concentration in brain tissue. As the results showed, T80-NPS-RIN traveled through BBB and delivered RIN to the brain. The findings confirmed that T80-NPS-RIN did not only cross the blood–brain barrier, but also provided better neuroprotective effects. The results indicated nanoparticles could promote the therapy of AD. In addition, T80-NPS-RIN did not cause hemolysis exhibiting good biocompatibility and could increase the effect of RIN in vivo according to the pharmacokinetic results. These results evidenced T80-NPS-RIN has great potential for AD therapy.

Table 1 Pharmacokinetic Parameters

Tissue	PK Parameter	RIN Solution	NPS-RIN	T80-NPS-RIN
Serum	C_{max} (ng/mL)*	164.4	536.3	673
	Cl (mL/h/kg)*	5912.78	2059.67	1938.76
	AUC (ng/mL hr)*	136.06	388.41	412.63
	$T_{1/2}$ (h)	1.14	1.28	1.48

Notes: *Statistically significant difference between treatment groups.

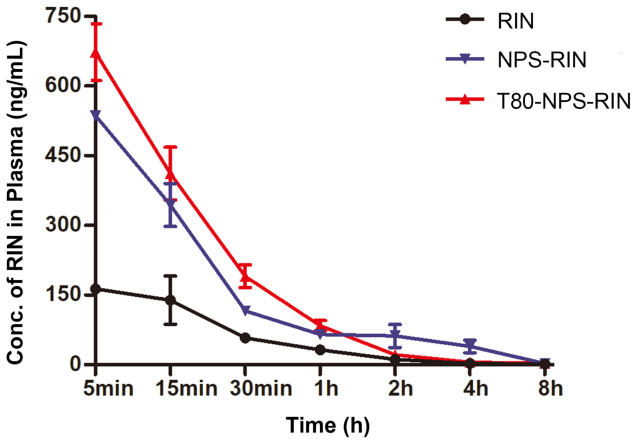

Figure 6 Pharmacokinetic profiles of free RIN, NPS-RIN and T80-NPS-RIN after intravenous injection (n=6). Plasma concentration–time curve of free RIN, NPS-RIN and T80-NPS-RIN nanoparticles.

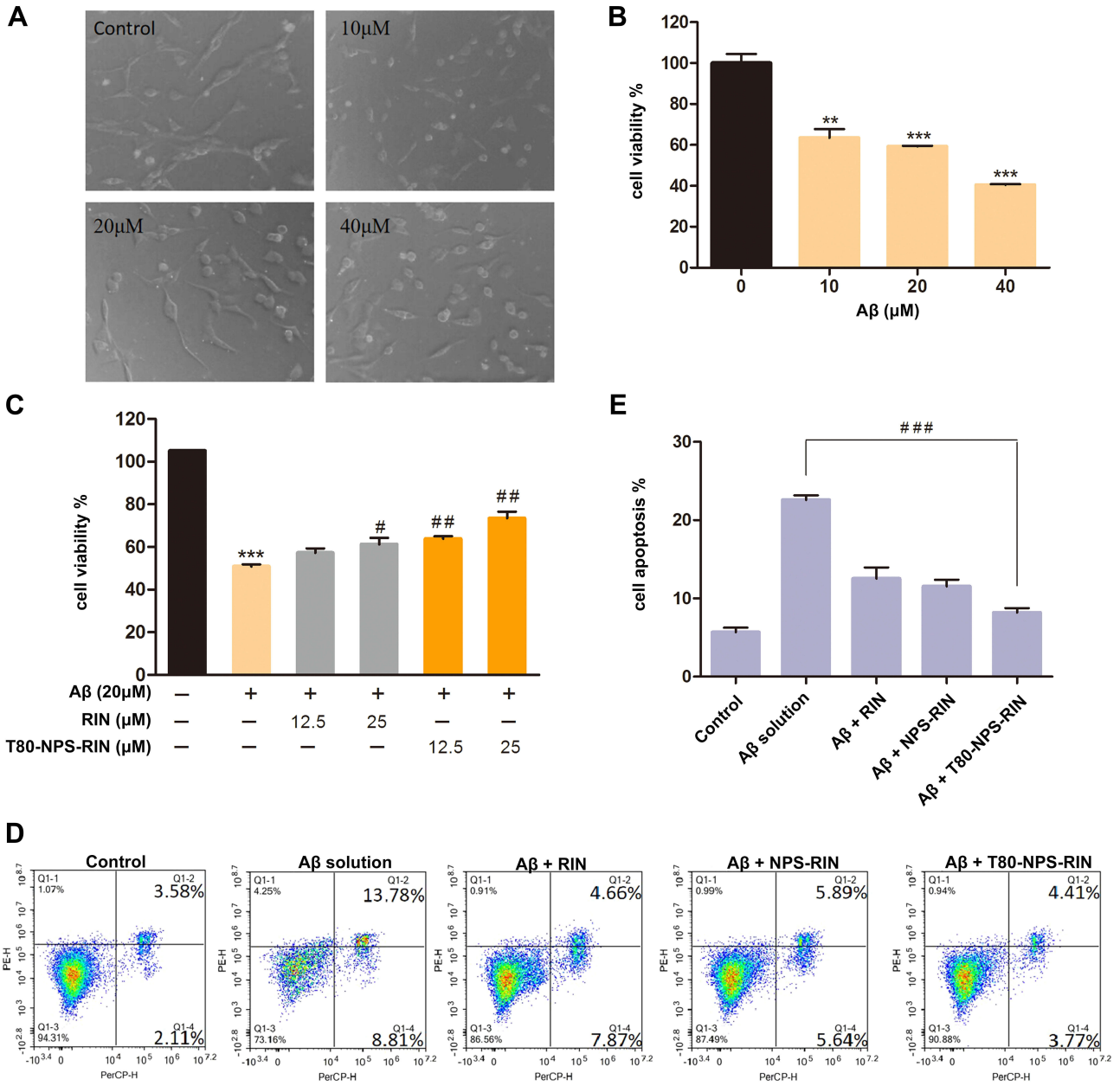

Figure 7 Drug treatment regulated the activity of neurons in vitro. (**A**) The images of PC12 cells injured by various concentrations of $A\beta_{25-35}$ solution. (**B**) The treatment of PC12 cells with $A\beta_{25-35}$ (10, 20, and 40 μM) alone for 24 hrs was represented by the MTT assay. (**C**) The inhibiting effects of RIN or T80-NPS-RIN (12.5 and 25 μM) were investigated through pretreatment for 4 hrs. (**D, E**) The effect of RIN, NPS-RIN and T80-NPS-RIN in $A\beta_{25-35}$-induced apoptosis PC12 cells were double-stained with Annexin V PE/7-AAD and analyzed by flow cytometry. Values were the mean ± SD (n = 3). **P < 0.01, and ***P < 0.001 compared to the control groups. $^{\#}$P < 0.05 and $^{\#\#}$P < 0.01 vs the Aβ group. $^{\#\#\#}$P < 0.001, T80-NPS-RIN compared with Aβ solution therapy.

Acknowledgment

This research was supported by Sichuan Province Natural Science Foundation (No.2019YFS0092).

Disclosure

The authors report no conflicts of interest in this work.

References

1. Scheltens P, Blennow K, Breteler MMB, et al. Alzheimer's disease. *Lancet*. 2016;388(10043):505–517. doi:10.1016/S0140-6736(15)01124-1
2. Congdon EE, Sigurdsson EM. Tau-targeting therapies for Alzheimer disease. *Nat Rev Neurol*. 2018;14(7):399–415. doi:10.1038/s41582-018-0013-z

3. Villemagne VL, Doré V, Burnham SC, et al. Imaging tau and amyloid-β proteinopathies in Alzheimer disease and other conditions. *Nat Rev Neurol*. 2018;14(4):225–236. doi:10.1038/nrneurol.2018.9
4. Feng Y, Yang S-G, Du X-T, et al. Ellagic acid promotes Ab42 fibrillization and inhibits Ab42-induced neurotoxicity. *Biochem Biophys Res Commun*. 2009;390(4):1250–1254. doi:10.1016/j.bbrc.2009.10.130
5. Boche D, Denham N, Holmes C, et al. Neuropathology after active Abeta42 immunotherapy: implications for Alzheimer's disease pathogenesis. *Acta Neuropathol*. 2010;120(3):369–384. doi:10.1007/s00401-010-0719-5
6. Selkoe DJ, Hardy J. The amyloid hypothesis of Alzheimer's disease at 25 years. *EMBO Mol Med*. 2016;8(6):595–608. doi:10.15252/emmm.201606210
7. Wang P, Zheng X, Guo Q, et al. Systemic delivery of BACE1 siRNA through neuron-targeted nanocomplexes for treatment of Alzheimer's disease. *J Controlled Release*. 2018;279:220–233. doi:10.1016/j.jconrel.2018.04.034
8. Agrawal M, Saraf S, Saraf S, et al. Nose-to-brain drug delivery: an update on clinical challenges and progress towards approval of anti-Alzheimer drugs. *J Controlled Release*. 2018;281:139–177. doi:10.1016/j.jconrel.2018.05.011
9. Zhang J, Yang C, Wei D, et al. Long-term efficacy of Chinese medicine bushen capsule on cognition and brain activity in patients with amnestic mild cognitive impairment. *Pharmacol Res*. 2019;146:104319. doi:10.1016/j.phrs.2019.104319
10. Lin HQ, Ho MT, Lau LS, Wong KK, Shaw PC, Wan DC. Anti-acetylcholinesterase activities of traditional Chinese medicine for treating Alzheimer's disease. *Chem Biol Interact*. 2008;175(1–3):352–354. doi:10.1016/j.cbi.2008.05.030
11. May BH, Lit M, Xue CC, et al. Herbal medicine for dementia: a systematic review. *Phytother Res*. 2009;23(4):447–459. doi:10.1002/ptr.2656
12. Yang WT, Zheng XW, Chen S, et al. Chinese herbal medicine for Alzheimer's disease: clinical evidence and possible mechanism of neurogenesis. *Biochem Pharmacol*. 2017;141:143–155. doi:10.1016/j.bcp.2017.07.002
13. Howes MJ, Perry NS, Houghton PJ. Plants with traditional uses and activities, relevant to the management of Alzheimer's disease and other cognitive disorders. *Phytother Res*. 2003;17(1):1–18. doi:10.1002/ptr.1280
14. Li C, Tu G, Luo C, et al. Effects of rhynchophylline on the hippocampal miRNA expression profile in ketamine-addicted rats. *Prog Neuro-Psychopharmacol Biol Psychiatry*. 2018;86:379–389. doi:10.1016/j.pnpbp.2018.02.009
15. Xian YF, Lin ZX, Zhao M, Mao QQ, Ip SP, Che CT. Uncaria rhynchophylla ameliorates cognitive deficits induced by D-galactose in mice. *Planta Med*. 2011;77(18):1977–1983. doi:10.1055/s-0031-1280125
16. Shao H, Mi Z, Ji WG, et al. Rhynchophylline protects against the amyloid beta-induced increase of spontaneous discharges in the hippocampal CA1 region of rats. *Neurochem Res*. 2015;40(11):2365–2373. doi:10.1007/s11064-015-1730-y
17. Fu AK, Hung KW, Huang H, et al. Blockade of EphA4 signaling ameliorates hippocampal synaptic dysfunctions in mouse models of Alzheimer's disease. *Proc Natl Acad Sci U S A*. 2014;111(27):9959–9964. doi:10.1073/pnas.1405803111
18. Zhang C, Wu X, Xian Y, Zhu L, Lin G, Lin ZX. Evidence on integrating pharmacokinetics to find truly therapeutic agent for Alzheimer's disease: comparative pharmacokinetics and disposition kinetics profiles of stereoisomers isorhynchophylline and rhynchophylline in rats. *Evid Based Complement Alternat Med*. 2019;2019:4016323. doi:10.1155/2019/4016323
19. Imamura S, Tabuchi M, Kushida H, et al. The blood-brain barrier permeability of geissoschizine methyl ether in Uncaria hook, a galenical constituent of the traditional Japanese medicine yokukansan. *Cell Mol Neurobiol*. 2011;31(5):787–793. doi:10.1007/s10571-011-9676-3
20. Wei H, Liu T, Jiang N, et al. A novel delivery system of cyclovirobuxine D for brain targeting: angiopep-conjugated polysorbate 80-coated liposomes via intranasal administration. *J Biomed Nanotechnol*. 2018;14(7):1252–1262. doi:10.1166/jbn.2018.2581
21. Zhang TT, Li W, Meng G, Wang P, Liao W. Strategies for transporting nanoparticles across the blood-brain barrier. *Biomater Sci*. 2016;4(2):219–229. doi:10.1039/c5bm00383k
22. Wang N, Sun P, Lv M, Tong G, Jin X, Zhu X. Mustard-inspired delivery shuttle for enhanced blood-brain barrier penetration and effective drug delivery in glioma therapy. *Biomater Sci*. 2017;5(5):1041–1050. doi:10.1039/c7bm00133a
23. Dibaei M, Rouini MR, Sheikholeslami B, Gholami M, Dinarvand R. The effect of surface treatment on the brain delivery of curcumin nanosuspension: in vitro and in vivo studies. *Int J Nanomed*. 2019;14:5477–5490. doi:10.2147/IJN.S199624
24. Saraiva C, Praca C, Ferreira R, Santos T, Ferreira L, Bernardino L. Nanoparticle-mediated brain drug delivery: overcoming blood-brain barrier to treat neurodegenerative diseases. *J Controlled Release*. 2016;235:34–47. doi:10.1016/j.jconrel.2016.05.044
25. Wilson B, Samanta MK, Santhi K, Kumar KP, Paramakrishnan N, Suresh B. Targeted delivery of tacrine into the brain with polysorbate 80-coated poly(n-butylcyanoacrylate) nanoparticles. *Eur J Pharm Biopharm*. 2008;70(1):75–84. doi:10.1016/j.ejpb.2008.03.009
26. Yang K, Hewarathna A, Geerlof-Vidavsky I, Rao VA, Gryniewicz-Ruzicka CM, Keire DA. Screening of Polysorbate-80 composition by high resolution mass spectrometry with rapid H/D exchange. *Anal Chem*. 2019;91:14649–14656. doi:10.1021/acs.analchem.9b03809
27. Gaucher G, Marchessault RH, Leroux JC. Polyester-based micelles and nanoparticles for the parenteral delivery of taxanes. *J Controlled Release*. 2010;143(1):2–12. doi:10.1016/j.jconrel.2009.11.012
28. Brown RC, Morris AP, O'Neil RG. Tight junction protein expression and barrier properties of immortalized mouse brain microvessel endothelial cells. *Brain Res*. 2007;1130(1):17–30. doi:10.1016/j.brainres.2006.10.083
29. Colgan OC, Collins NT, Ferguson G, et al. Influence of basolateral condition on the regulation of brain microvascular endothelial tight junction properties and barrier function. *Brain Res*. 2008;1193:84–92. doi:10.1016/j.brainres.2007.11.072
30. Dohgu S, Banks WA. Lipopolysaccharide-enhanced transcellular transport of HIV-1 across the blood-brain barrier is mediated by the p38 mitogen-activated protein kinase pathway. *Exp Neurol*. 2008;210(2):740–749. doi:10.1016/j.expneurol.2007.12.028
31. Sun W, Xie C, Wang H, Hu Y. Specific role of polysorbate 80 coating on the targeting of nanoparticles to the brain. *Biomaterials*. 2004;25(15):3065–3071. doi:10.1016/j.biomaterials.2003.09.087